



This is a repository copy of *Limits on WIMP cross-sections from the NAIAD experiment at the Boulby underground laboratory*.

White Rose Research Online URL for this paper:
<http://eprints.whiterose.ac.uk/120282/>

Version: Submitted Version

Article:

Ahner, G.J., Araujo, H.M., Arnison, G.J. et al. (46 more authors) (2005) Limits on WIMP cross-sections from the NAIAD experiment at the Boulby underground laboratory. *Physics Letters B*, 616 (1-2). pp. 17-24. ISSN 0370-2693

<https://doi.org/10.1016/j.physletb.2000.09.001>

Reuse

This article is distributed under the terms of the Creative Commons Attribution-NonCommercial-NoDerivs (CC BY-NC-ND) licence. This licence only allows you to download this work and share it with others as long as you credit the authors, but you can't change the article in any way or use it commercially. More information and the full terms of the licence here: <https://creativecommons.org/licenses/>

Takedown

If you consider content in White Rose Research Online to be in breach of UK law, please notify us by emailing eprints@whiterose.ac.uk including the URL of the record and the reason for the withdrawal request.



eprints@whiterose.ac.uk
<https://eprints.whiterose.ac.uk/>

Limits on WIMP cross-sections from the NAIAD experiment at the Boulby Underground Laboratory

The UK Dark Matter Collaboration

G. J. Alner ^a, H. M. Araújo ^b, G. J. Arnison ^a, J. C. Barton ^{c 1},
 A. Bewick ^b, C. Bungau ^b, B. Camanzi ^b, M. J. Carson ^d, D. Davidge ^b,
 E. Daw ^d, J. V. Dawson ^b, G. J. Davies ^b, J. C. Davies ^d, C. Duffy ^d,
 T. J. Durkin ^a, T. Gamble ^d, S. P. Hart ^a, R. Hollingworth ^d,
 G. J. Homer ^a, A. S. Howard ^b, I. Ivaniouchenkov ^{a,b}, W. G. Jones ^b,
 M. K. Joshi ^b, J. Kirkpatrick ^d, V. A. Kudryavtsev ^{d 2}, T. B. Lawson ^d,
 V. Lebedenko ^b, M. J. Lehner ^{d 3}, J. D. Lewin ^a, P. K. Lightfoot ^d,
 I. Liubarsky ^b, R. Lüscher ^{a,b}, J. E. McMillan ^d, B. Morgan ^d,
 A. Murphy ^e, A. Nickolls ^a, G. Nicklin ^d, S. M. Paling ^d,
 R. M. Preece ^a, J. J. Quenby ^b, J. W. Roberts ^{a,d}, M. Robinson ^d,
 N. J. T. Smith ^a, P. F. Smith ^a, N. J. C. Spooner ^{d 4}, T. J. Sumner ^b,
 D. R. Tovey ^d, E. Tziaferi ^d

^a *Particle Physics Department, Rutherford Appleton Laboratory,
 OX11 0QX, UK*

^b *Blackett Laboratory, Imperial College London, SW7 2BZ, UK*

^c *Department of Physics, Queen Mary – University of London, E1 4NS, UK*

^d *Department of Physics and Astronomy, University of Sheffield, S3 7RH, UK*

^e *School of Physics, University of Edinburgh, EH9 3JZ, UK*

Abstract

The NAIAD experiment (NaI Advanced Detector) for WIMP dark matter searches at the Boulby Underground Laboratory (North Yorkshire, UK) ran from 2000 until 2003. A total of 44.9 kg×years of data collected with 2 encapsulated and 4 unencapsulated NaI(Tl) crystals with high light yield were included in the analysis. We present final results of this analysis carried out using pulse shape discrimination. No signal associated with nuclear recoils from WIMP interactions was observed in any run with any crystal. This allowed us to set upper limits on the WIMP-nucleon spin-independent and WIMP-proton spin-dependent cross-sections. The NAIAD experiment has so far imposed the most stringent constraints on the spin-dependent WIMP-proton cross-section.

¹deceased

²Corresponding author, e-mail: v.kudryavtsev@sheffield.ac.uk

³Now at the University of Pennsylvania, Philadelphia, PA 19104, USA

⁴Corresponding author, e-mail: n.spooner@sheffield.ac.uk

Key words: Dark matter, WIMP, neutralino, Pulse shape analysis, Scintillation detectors, Inorganic crystals

PACS: 95.35.+d, 95.30.Cq, 14.80.Ly, 29.40.Mc

Corresponding author: V. A. Kudryavtsev, N. J. C. Spooner, Department of Physics and Astronomy, University of Sheffield, Hicks Building, Hounsfield Rd., Sheffield S3 7RH, UK

Tel: +44 (0)114 2224531;

Fax: +44 (0)114 2728079;

E-mail: v.kudryavtsev@sheffield.ac.uk, n.spooner@sheffield.ac.uk

1. Introduction

The UK Dark Matter Collaboration (UKDMC) has been operating various detectors for non-baryonic dark matter searches at the Boulby Underground Laboratory (North Yorkshire, UK) for many years. Limits on the flux of weakly interacting massive particles (WIMPs) – the primary candidate for the non-baryonic dark matter that may constitute up to 90% of the mass of the Galaxy, were set using data from the first NaI(Tl) detector [1, 2] and later improved with an array of several NaI(Tl) crystals (NAIAD) [3]. Pulse shape analysis (PSA) was applied to the data to distinguish between slow scintillations arising from background electron recoils and fast scintillations due to nuclear recoils, which are expected from WIMP-nucleus interactions [4].

The advance of the UKDMC NaI(Tl) experiment was blocked for a few years (1997-2000) by the discovery of a fast anomalous component in the data from several encapsulated crystals [5]. These events were faster than typical electron recoil pulses and faster even than nuclear recoil pulses [5, 6]. Similar events were also seen by the Saclay group [7]. These events were later shown to be due to implanted surface contamination of the crystal by an alpha-emitting isotope from radon decay [8, 9].

NAIAD was constructed in 2000-2001 with 5 unencapsulated crystals to allow better control of the crystal surface, to reduce the background due to surface events and to improve the light collection [3, 10]. In 2002 two more encapsulated crystals were added to the array.

Despite the limited sensitivity of inorganic scintillators to WIMP interactions, interest in the NaI(Tl) crystals has remained high for the past several years because of the DAMA group's claim of an annual modulation in their NaI(Tl) array consistent with the expected signal from WIMP-nucleus interactions with a specific set of WIMP parameters [11].

NaI has the advantage of having two target nuclei with high and low masses, thus reducing uncertainties related to nuclear physics calculations. The detectors are sensitive to both spin-independent and spin-dependent interactions. The NAIAD experiment is complementary to other dark matter experiments at Boulby, such as ZEPLIN [12] (liquid xenon and two phase xenon detectors) and DRIFT [13] (time projection chamber with directional sensitivity). The array of NaI(Tl) detectors was also used as a diagnostic array to study background and systematic effects for other experiments at Boulby.

First results from the NAIAD experiment (10.6 kg×years exposure from 2000-2001) were published in Ref. [3]. Preliminary limits from an extended set of data (combined with the previous set) with total exposure of 20.3 kg×years (2000-2002) were set in Ref. [14]. In this paper we present results from the NAIAD experiment based on all data sets collected in 2000-2003.

2. The NAIAD experiment

The NAIAD array was sited in the underground laboratory at Boulby mine at a vertical depth of 1070 metres or 2805 m w. e. [15]. It consisted of 7 NaI(Tl) crystals from different manufacturers (Bicron, Hilger, VIMS and Crismatec–Saint-Gobain) with a total mass of about 55 kg. Two detectors contained encapsulated crystals, while 5 other crystals were unencapsulated. To avoid their degradation by humidity in the atmosphere, the unencapsulated crystals were sealed in copper boxes filled with dry

nitrogen.

One of the crystals (DM70-Saclay) of similar design to those used by the DAMA group in its 100 kg array, was previously running at Modane and then moved to Boulby in 2001. When encapsulated, it showed the anomalous fast population of events [7, 9], which were explained as being due to implanted surface contamination of the crystal by an alpha-emitting isotope from radon decay [8, 9]. It was de-encapsulated in 2002, polished and was running as part of the NAIAD array in 2002-2003. No fast population was seen in the crystal after de-encapsulation [16, 17].

Each crystal was mounted in a 10 mm thick solid PTFE (polytetrafluoroethylene) reflector cage and was coupled to light guides. The two 4-5 cm long quartz light guides were also mounted in the PTFE cages and were coupled to 5 inch diameter low background photomultiplier tubes (PMTs), ETL type 9390UKB. Only selected low background materials were used in the detector design including oxygen-free high-conductivity copper and PTFE.

Temperature control of the system was achieved through copper coils outside the copper box. Chilled water was constantly pumped through the coils maintaining the temperature of the crystals stable to within a fraction of a degree during a single run. The temperature of the crystal, ambient air, water in the pipes and copper was measured by thermocouples. If, for any reason (for example, chiller failure), the variation of crystal temperature exceeded the predefined limit, the data from these periods were not included in the analysis. If any changes in the experimental set-up resulted in a change of the mean temperature of the crystal, the data from different runs were not combined together, but assumed to come from different experiments, so only the resulting limits were combined.

Pulses from individual PMTs were integrated using a buffer circuit and then digitised using an Acqiris CompactPCI based data acquisition (DAQ) system. Note that previous results [3] were obtained with a digital oscilloscope and Labview-based DAQ software. The digitised pulse shapes (5 μ s total digitisation time, 10 ns digitisation accuracy) were passed to a computer running Linux OS and stored on disk. The gain of the PMTs was set to give about 2.5 mV per photoelectron. Low threshold discriminators were set to about 10 mV threshold, which corresponded to about 1-1.5 keV of electron equivalent energy. A software threshold was set at 4 keV since no pulse shape discrimination was observed below this energy [3].

Copper boxes containing the crystals were installed in lead and copper “castles”, to shield the detectors from background due to natural radioactivity in the surrounding rock. Wax and polypropylene neutron shielding (about 10 g/cm²) around the castles was installed in Spring 2002 and all data presented here (2002-2003) were collected with neutron shielding in place.

The light yield of the crystals was obtained from measurement of the single photoelectron pulses and the energy calibration with a 122 keV ⁵⁷Co gamma-ray source. The crystals had light yields of 4.6-8.4 pe/keV. The large difference in the crystal light yield is not surprising taking into account the different origin (manufacturers) of the crystals, encapsulation, reflecting material, size of the light guides and PMT response. The light yield was checked every 2-4 weeks and was found to be stable within 10% for all crystals over long running periods (several months and more). The longest operated unencapsulated crystal, running since the summer of 2000, showed a degradation in light yield of no more than 10%. Small variations in the light yield do not affect the

energy threshold for the data analysis since it is significantly higher (4 keV) than the effective hardware threshold (typically less than 2 keV). Possible short term variations in the light yield, as well as any electronic problems (stability of the discriminator thresholds, high-voltage power supplies etc.) were monitored by plotting the energy spectra of gamma calibration data and real data for each day of running and removing suspicious data from the analysis. Any variations in the experimental conditions, mentioned above, would manifest themselves in the energy spectra.

3. Analysis procedure

Final analysis was performed on the sum of the pulses from the two PMTs attached to each crystal. The parameters of the pulses from each PMT were used to apply various cuts to remove the noise events from the analysis. Our standard procedure of data analysis involved fitting a single exponential to each integrated pulse in order to obtain the index of the exponential, τ , the amplitude of the pulse, A , and the start time, t_s . The scintillation pulses from nuclear and electron recoils were shown to be nearly exponential in shape [4]. In addition to these, the mean time of the pulse (mean photoelectron arrival time), as an estimate of the time constant, χ^2 of the fit, number of photoelectrons and the energy were also calculated for each pulse. Conversion of the pulse amplitude to the number of photoelectrons and the energy was achieved using pre-determined conversion factors, which come from energy and single photoelectron calibrations. These calibrations were performed typically every 2-4 weeks to ensure that there were no changes in the PMT gains or crystal degradation. Calibration with various gamma-ray sources provided the energy resolution of crystals [3].

For each run (or set of runs) the “energy – time constant” ($E - \tau$) distribution was constructed. If all operational settings (including temperature) were the same for several runs, the ($E - \tau$) distributions for these runs were summed together. Data collected at crystal temperatures outside a predefined range were removed from the analysis. Each event stored on the computer disk, had a temperature record in it. The mean daily temperature of each crystal was plotted as a function of time, and the mean temperature for a particular data set was calculated. The most common reason for a temperature to fluctuate significantly (several degrees) from the mean value was chiller failure. Data collected without cooling were removed from the analysis. When a broken chiller was replaced or repaired, it was impossible to achieve the same crystal temperature. In this case we considered the two data sets collected at different temperatures as independent and did not combine the data but only the final limits [3].

To reduce PMT noise and, particularly, events where a spark (flash) in the dynode structure of one PMT was seen by both PMTs, various cuts described in details in [16, 18] were applied. These cuts are an improvement upon those used in Ref. [3], having been shown to reject spurious events more efficiently while retaining a larger fraction of genuine scintillation pulses [16, 18]. The noise cuts were developed based on the experiment with two PMTs mounted face to face without the crystal between them. They were shown to cut similar fraction of scintillation pulses from electron and nuclear recoils (to within 2%) [16, 18]. The cut efficiency for nuclear recoil events from the surface calibration ranges from 84% at 4-6 keV up to almost 100% above 10 keV [16, 18] for one of the crystals. As these cuts were found to be similar (to within 2%)

for electron and nuclear recoils, the cut efficiencies for each particular crystal and data set were determined from the daily calibrations with the ^{60}Co gamma source. This also allowed the monitoring of the stability of these cuts.

For any small energy bin (1 keV width, for example), the time constant distribution was approximated by a Gaussian in $\ln(\tau)$ (log(Gauss) function) [3, 1, 6, 19] with three free parameters: mean time constant τ_o , width w and normalisation factor N_o . In experiments where a second population is seen (for example, nuclear recoils from a neutron source or possible WIMP-nucleus interactions), the resulting τ -distribution was fitted with two log(Gauss) functions with the same width w , since the width is determined mainly by the number of collected photoelectrons.

The aim of the analysis procedure was to find a second population of events in the τ -distributions or to set an upper limit on its rate. To reach this, the τ -distributions for all energies of interest (2-40 keV) were obtained for all crystals with gamma-ray (^{60}Co) and neutron (^{252}Cf) sources. Photons from high-energy gamma-ray sources produce Compton electrons in the crystal volume similar to those initiated by gamma-ray background in the crystal. Neutrons collide elastically with the nuclei of the crystal giving nuclear recoils similar to those expected from WIMP-nucleus elastic scattering. Calibrations were performed on all crystals at the surface prior to moving the crystals underground and were described in detail in Refs. [3, 6].

The crystal temperature and the light yield are the most important parameters which affect the time constant distributions and, finally, the results of the experiment. The temperature affects the pulse shape – mean time of the pulse and the index of an exponential. Increasing temperature causes the mean time (and the index of the fitted exponential) to decrease at a rate of about 5 ns per 1°C . If the temperature of the crystal is not stable, then combining data collected over a long period of time, we will broaden the time constant distribution. The same effect is observed if the light yield is not stable. To improve the quality of the data, the crystal temperature was controlled and monitored. To compensate for any small variations of the crystal temperature and light yield over long periods of time (several months) the gamma calibration of the crystal was done every day for 2 hours with the ^{60}Co gamma-ray source. In this way, any variation in the mean time constant and width of the time constant distributions of the real data, due to the effects mentioned above, is repeated in similar distributions constructed with gamma calibration data and used to fix some parameters in the fitting procedure (see Ref. [3] for a full description of the data analysis procedure). Note that the ratio of mean time constant for nuclear recoils to that of electron recoils does not depend on temperature [3] and was taken from the surface calibrations.

4. Results and discussion

The data from 6 crystals were used to set the limits on WIMP-nucleus cross-section reported here. One crystal was excluded from the data analysis due to its small mass (4 kg) and high background rate (about 15 events/kg/day/keV). Table 1 shows the main characteristics and statistics for all detectors for years 2002-2003. Statistics for the 10.6 kg \times years of data collected in the period 2000-2001 are to be found in Ref. [3].

An energy range from 4 to 10 keV was used in the data analysis. Previous results [3] were obtained for the energy range 4-30 keV. The smaller energy range in the present analysis was due to the smaller amplitude range set on the 8-bit waveform digitisers. A

total of 256 digitisation points for a smaller amplitude range allowed a more accurate calculation of the amplitude and time constant for single pulses at low energies and better noise suppression.

Figure 1 shows typical time constant distributions at 5-6 keV from data (before and after cuts) and a calibration run with gamma-ray source (after cuts). PMT noise events are seen at small values of time constant before cuts but are absent after the cuts were applied. Figure 1 does not reveal any visible difference between data and calibration runs in terms of time constant distributions. Limits on the nuclear recoil rate at any particular energy were obtained by fitting the measured time constant distribution with two log(Gauss) functions having known parameters: mean time constants and widths, known from Compton and neutron calibrations. Free parameters were the total numbers of electron and nuclear recoils (see Ref. [3] for further details). When both positive and negative values for the numbers of nuclear and electron recoils were allowed, the best fit values for nuclear recoil rates were either positive or negative but normally within 1.5 standard deviations from zero. Total event rates and nuclear recoil rates extracted from the best two log-Gaussian fits to the data are shown in Figure 2 for two runs with crystal DM74. The error bars for nuclear recoil rates correspond to 90% C.L. As can be seen, in none of the energy bins does the nuclear recoil rate deviate significantly from zero. Hence no contribution from WIMP-nucleus interactions were observed in these data. This was found to be true for all crystals. Since negative values are non-physical, to set upper limits on nuclear recoil rates we restricted the rates to non-negative values and carried out a two component fitting to the time constant distributions. To derive an upper limit at 90% C.L. we set the value of $\Delta(\chi^2) = \chi_{up}^2 - \chi_{min}^2 = 2.7$. Strictly speaking this $\Delta(\chi^2)$ corresponds to the 90% C.L. only if the number of searched events is equal to 0. For negative values of best fit number of nuclear recoils the value for an upper limit obtained in this analysis is higher than suggested in Ref. [20] where a unified approach to confidence intervals was discussed for the Gaussian-with-boundary problem. For positive values of best fit number of nuclear recoils we used the number of recoils at χ_{up}^2 as an estimate for an upper limit, which again gave us a higher value than would follow from Ref. [20]. Our approach was thus conservative and allowed us to avoid complications with different approaches suggested by different authors (see Ref. [20] and references therein for discussion). In this way, the upper limits on the nuclear recoil rate were obtained for each energy bin and for each crystal.

The limits obtained on the nuclear recoil rate for each energy bin and each crystal were converted into limits on the WIMP-nucleon spin-independent and WIMP-proton spin-dependent cross-sections following the procedure described by Lewin and Smith [21] and used previously in Ref. [3]. Expected nuclear recoil spectra from WIMP-nucleus interactions were calculated for a model with spherical isothermal dark matter halo with parameters: $\rho_{dm} = 0.3 \text{ GeV cm}^{-3}$, $v_o = 220 \text{ km/s}$, $v_{esc} = 600 \text{ km/s}$ and $v_{Earth} = 232 \text{ km/s}$. For the spin-independent case the form factors were computed using Fermi nuclear density distribution with the parameters to fit muon scattering data as described in Ref. [21]. The WIMP-nucleus scattering cross-section was taken proportional to A^2 . For the spin-dependent case a pure higgsino was assumed. The spin factors and form factors were computed for sodium and iodine nuclei on the basis of nuclear shell model calculations [22] with Bonn A potential. The quenching factors (scintillation efficiencies for nuclear recoils with respect to that for electron recoils)

were taken as 0.275 for sodium and 0.086 for iodine recoils [4].

The limits on the cross-section for various energy bins, targets (sodium and iodine) and crystals were combined following the procedure described in Ref. [21] and used previously in Ref. [3], assuming the measurements for different energy bins and different crystals were statistically independent.

Figure 3a (3b) shows the NAIAD limits on WIMP-nucleon spin-independent (WIMP-proton spin-dependent) cross-sections as functions of WIMP mass based on the data described in Table 1. Also shown in Figure 3a is the region of parameter space favoured by the DAMA positive annual modulation signal [11].

Model-independent limits on spin-dependent WIMP-proton and WIMP-neutron cross-sections, calculated following the procedure described in Ref. [23], are presented in Figure 4. The NAIAD experiment imposes the most stringent constraints so far on the spin-dependent WIMP-proton cross-section (see Refs. [24, 25] for a compilation of recent results).

5. Conclusions

Results from the NAIAD experiment for WIMP dark matter search at Boulby mine were presented. Pulse shape analysis was used to discriminate between nuclear recoils, possibly caused by WIMP interactions, and electron recoils due to gamma-ray background. We obtained upper limits on the WIMP-nucleon spin-independent and WIMP-proton spin-dependent cross-sections based on the data accumulated by 6 modules (44.9 kg×years exposure). The NAIAD experiment imposes the most stringent constraints so far on spin-dependent WIMP-proton cross-section.

6. Acknowledgements

The Collaboration wishes to thank PPARC for financial support. We are grateful to the staff of Cleveland Potash Ltd. for assistance. We would also like to thank Prof. G. Gerbier, Drs. J. Mallet, L. Mosca (Saclay), and Dr. C. Tao (CPPM, Marseille) for providing us with one of their crystals for the NAIAD experiment. C. Duffy work was supported by the Nuffield Foundation through the Undergraduate Research Bursary in Science. We also acknowledge the funding from EU FP6 programme – ILIAS.

References

- [1] P. F. Smith et al. *Physics Letters B*, **379** (1996) 299.
- [2] J. Quenby et al. *Astroparticle Physics* **5** (1996) 249.
- [3] B. Ahmed et al. (The UK Dark Matter Collaboration). *Astroparticle Physics*, **19** (2003) 691.
- [4] D. R. Tovey et al. *Physics Letters B*, **433** (1998) 150.
- [5] P. F. Smith et al. *Physics Reports*, **307** (1998) 275.
- [6] V. A. Kudryavtsev et al. *Physics Letters B*, **452** (1999) 167.

- [7] G. Gerbier et al. *Astroparticle Physics* **11** (1999) 287.
- [8] N. J. T. Smith, J. D. Lewin and P. F. Smith. *Physics Letters B*, **485** (2000) 9.
- [9] V. A. Kudryavtsev et al. *Astroparticle Physics*, **17** (2002) 401.
- [10] N. J. C. Spooner et al. *Physics Letters B*, **473** (2000) 330.
- [11] R. Bernabei et al. *Physics Letters B*, **480** (2000) 23.
- [12] G. J. Alner et al. (The UK Dark Matter Collaboration). *Astroparticle Physics*, in press.
- [13] G. J. Alner et al. *Nucl. Instrum. and Meth. in Phys. Res. A*, **535** (2004) 644.
- [14] M. Carson (for the UK Dark Matter Collaboration). *Proc. of the 28th Intern. Cosmic Ray Conf.* (Tsukuba, Japan, 31 July – 7 August, 2003), HE3.3: <http://www-rccn.icrr.u-tokyo.ac.jp/icrc2003/PROCEEDINGS/PDF/420.pdf>.
- [15] M. Robinson et al. *Nucl. Instrum. and Meth. in Phys. Res. A*, **511** (2003) 347.
- [16] M. Robinson. PhD Thesis, University of Sheffield, 2003.
- [17] M. Robinson et al., in preparation.
- [18] M. Robinson et al. *Nucl. Instrum. and Meth. in Phys. Res. A*, in press; physics/0503044.
- [19] D. R. Tovey. PhD Thesis, University of Sheffield (1998).
- [20] R. D. Cousins. *Phys. Rev. D*, **62** (2000) 098301; physics/0001031.
- [21] J. D. Lewin and P. F. Smith. *Astroparticle Physics* **6** (1996) 87.
- [22] M. T. Ressell and D. J. Dean. *Phys. Rev. C*, **56** (1997) 535.
- [23] D. R. Tovey et al. *Physics Letters B*, **488** (2000) 17.
- [24] A. Benoit et al. (The EDELWEISS Collaboration), astro-ph/0412061.
- [25] F. Giuliani. *Phys. Rev. Lett.*, **93** (2004) 161301.

Table 1: Statistics for NAIAD detectors running during years 2002-2003.

Crystal	Mass, kg	Light yield, pe/keV	Time, days	Exposure, kg×days
DM70-Saclay	10.0	5.1 ± 0.4	157.2	1571.7
DM74	8.40	8.4 ± 0.4	298.3	2505.4
DM76	8.32	4.6 ± 0.3	131.0	1089.6
DM77	8.41	6.1 ± 0.3	221.9	1866.2
DM80	8.47	8.0 ± 0.5	312.0	2642.7
DM81	8.47	6.6 ± 0.4	336.2	2847.2
Total exposure				12523

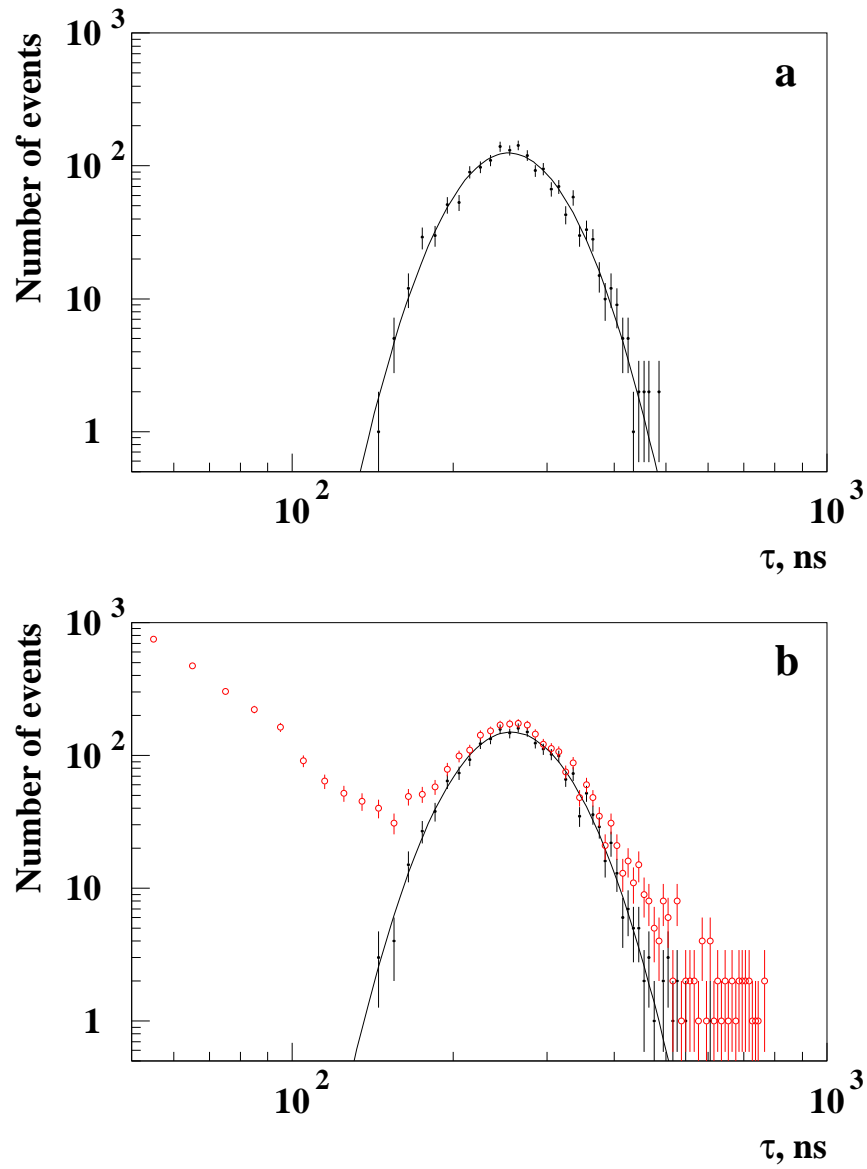


Figure 1: Typical time constant distributions (shown here for crystal DM74) at energies 5-6 keV: *a* – for gamma calibration run (after cuts), *b* – for data before (open circles) and after (filled circles) cuts.

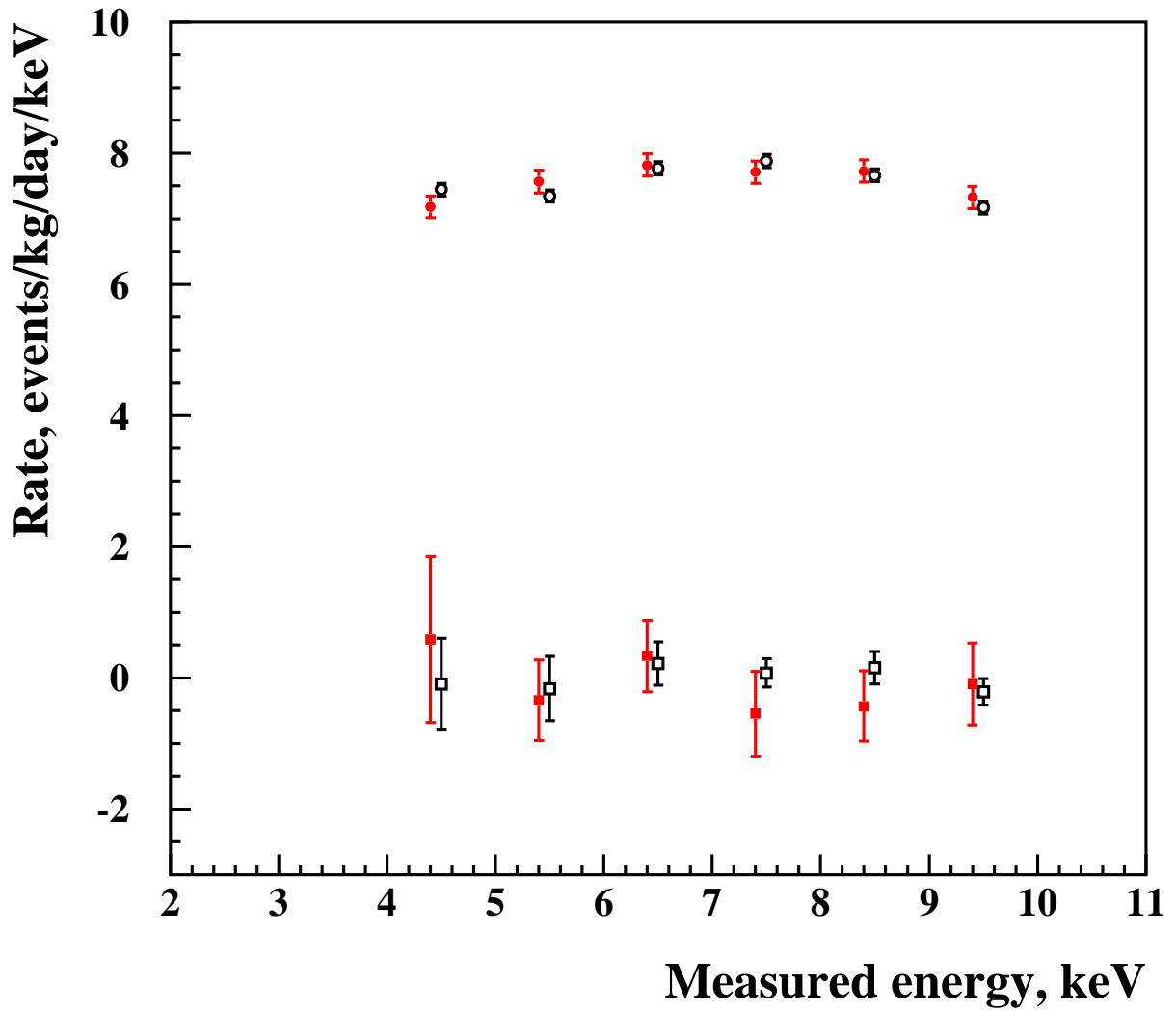


Figure 2: Energy spectra after cuts from two runs of one of the crystals (DM74) (filled and open circles) and the nuclear recoil rate for various energy bins (filled and open squares) with error bars drawn at 90% C.L. Energy bins are: 4-5 keV, 5-6 keV, etc. The points are shifted with respect to each other along x-axis to avoid overlapping.

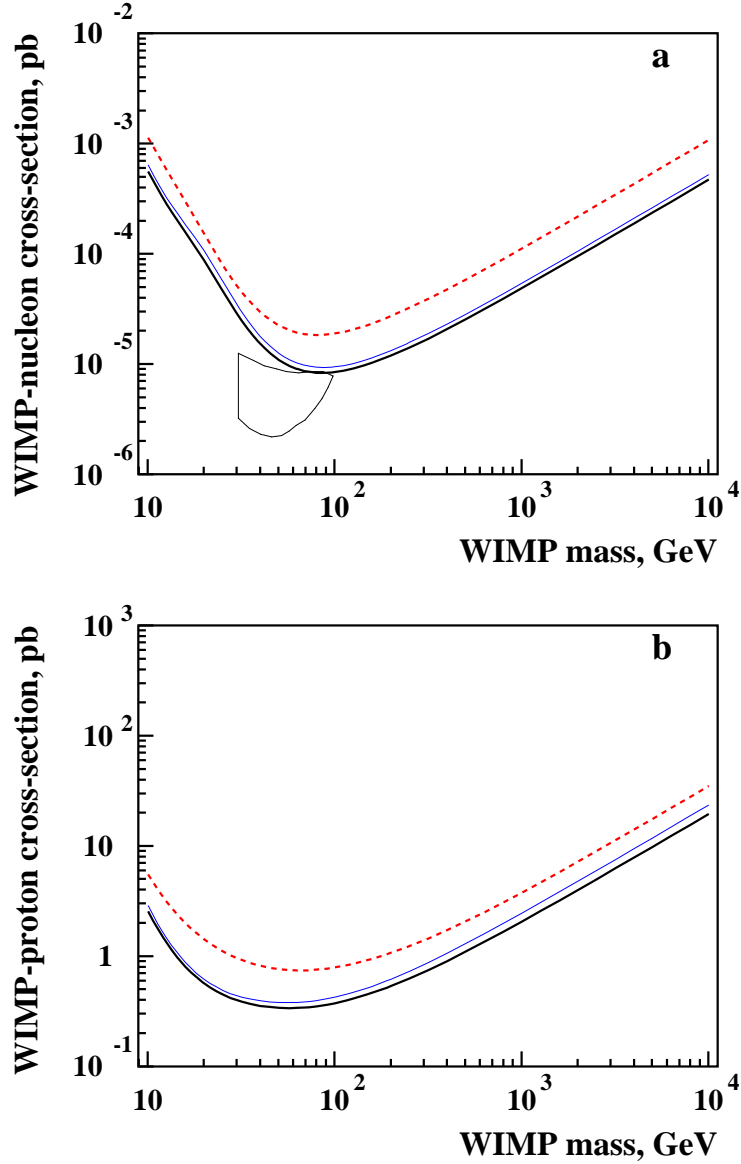


Figure 3: NAIAD limits (90% C.L.) on WIMP-nucleon spin-independent (a) and WIMP-proton spin-dependent (b) cross-sections as functions of WIMP mass: dashed curves – previously published limit [3], thin solid curves – limit from 2002-2003 data, thick solid curves – combined limit (2000-2003). Also shown is the region of parameter space favoured by the claimed DAMA positive annual modulation signal (DAMA/NaI-1 through DAMA/NaI-4) (closed curve).

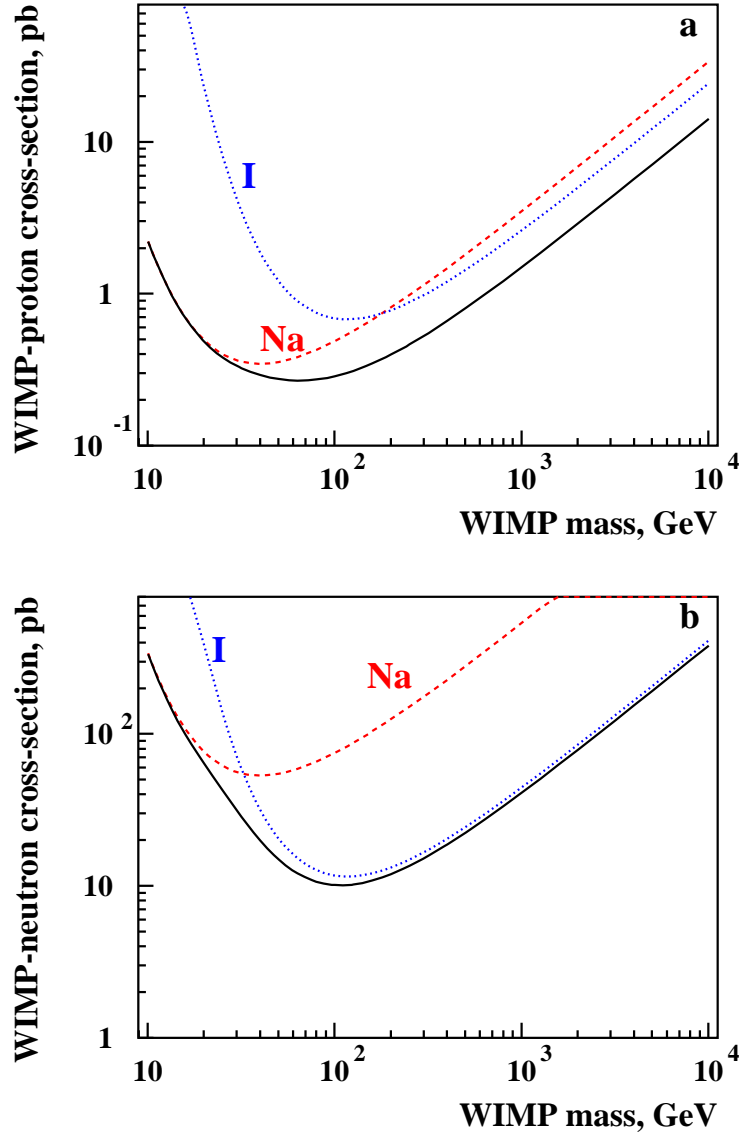


Figure 4: Model-independent limits (90% C.L.) on spin-dependent WIMP-proton (a) and WIMP-neutron (b) cross-sections as functions of WIMP mass. The limits were derived following the procedure described in Ref. [23]. Dashed curves show the limits extracted from interactions with sodium, dotted curves show those from iodine, and solid curves show combined limits.